Regional Fractional Ventilation by Using Multibreath Wash-in ^{3}He MR Imaging[1]

Hooman Hamedani, MS
Justin T. Clapp, PhD
Stephen J. Kadlecek, PhD
Kiarash Emami, PhD[2]
Masaru Ishii, MD, PhD[3]
Warren B. Gefter, MD
Yi Xin, MS
Maurizio Cereda, PhD
Hoora Shaghaghi, PhD
Sarmad Siddiqui, BS
Milton D. Rossman, MD
Rahim R. Rizi, PhD

Purpose: To assess the feasibility and optimize the accuracy of the multibreath wash-in hyperpolarized helium 3 (^{3}He) approach to ventilation measurement by using magnetic resonance (MR) imaging as well as to examine the physiologic differences that this approach reveals among nonsmokers, asymptomatic smokers, and patients with chronic obstructive pulmonary disease (COPD).

Materials and Methods: All experiments were approved by the local institutional review board and compliant with HIPAA. Informed consent was obtained from all subjects. To measure fractional ventilation, the authors administered a series of identical normoxic hyperpolarized gas breaths to the subject; after each inspiration, an image was acquired during a short breath hold. Signal intensity buildup was fit to a recursive model that regionally solves for fractional ventilation. This measurement was successfully performed in nine subjects: three healthy nonsmokers (one man, two women; mean age, 45 years ± 4), three asymptomatic smokers (three men; mean age, 51 years ± 5), and three patients with COPD (three men; mean age, 59 years ± 5). Repeated measures analysis of variance was performed, followed by post hoc tests with Bonferroni correction, to assess the differences among the three cohorts.

Results: Whole-lung fractional ventilation as measured with hyperpolarized ^{3}He in all subjects (mean, 0.24 ± 0.06) showed a strong correlation with global fractional ventilation as measured with a gas delivery device ($R^2 = 0.96$, $P < .001$). Significant differences between the means of whole-lung fractional ventilation ($F_{2,10} = 7.144$, $P = .012$) and fractional ventilation heterogeneity ($F_{2,10} = 7.639$, $P = .010$) were detected among cohorts. In patients with COPD, the protocol revealed regions wherein fractional ventilation varied substantially over multiple breaths.

Conclusion: Multibreath wash-in hyperpolarized ^{3}He MR imaging of fractional ventilation is feasible in human subjects and demonstrates very good global (whole-lung) precision. Fractional ventilation measurement with this physiologically realistic approach reveals significant differences between patients with COPD and healthy subjects. To minimize error, several sources of potential bias must be corrected when calculating fractional ventilation.

©RSNA, 2016

Online supplemental material is available for this article.

[1] From the Department of Radiology (H.H., J.T.C., S.J.K., K.E., M.I., W.B.G., Y.X., H.S., S.S., R.R.R.), Department of Anesthesiology and Critical Care (M.C.), and Pulmonary, Allergy and Critical Care Division (M.D.R.), University of Pennsylvania, 308 Stemmler Hall, 3450 Hamilton Walk, Philadelphia, PA 19104. Received March 5, 2015; revision requested April 21; revision received June 29; accepted July 27; final version accepted October 16. **Address correspondence to** R.R.R. (e-mail: *Rahim.Rizi@uphs.upenn.edu*).

[2] **Current address:** Polarean, Inc, Research Triangle Park, NC.

[3] **Current address:** Department of Otolaryngology-Head and Neck Surgery, Johns Hopkins University, Baltimore, Md.

Although a degree of regional variability in ventilation is typical in healthy subjects (1), regions where ventilation is reduced or completely absent are significantly more prevalent in subjects with obstructive lung diseases (2). One approach for assessing disease-related alterations in regional ventilation has been static single-breath magnetic resonance (MR) imaging with hyperpolarized helium 3 (^{3}He), which has been used to investigate chronic obstructive pulmonary disease (COPD) (3), asthma (4), and cystic fibrosis (5,6), among other lung disorders. This technique has been shown to outperform spirometry in its sensitivity and predictive power (7). However, despite the promising diagnostic potential of hyperpolarized gas ventilation measurement, imaging the lungs after a single breath does not give the inspired gas the opportunity to enter slow-filling regions (8), limiting the information that can be obtained with this approach.

To obtain an assessment of regional ventilation that reflects intrinsic pulmonary physiology, investigators have begun to develop dynamic hyperpolarized gas techniques that image subjects over several breathing cycles. Multibreath ^{3}He ventilation imaging was initially implemented by Deninger et al (9) in guinea pigs by using analysis of signal intensity wash-in over several breathing cycles, which required very large amounts of ^{3}He and long acquisition times. Emami et al (10) reduced the use of gas and the duration of the protocol by implementing a wash-in ventilation sequence in pigs whereby an image was obtained after each breath over the multibreath sequence. Recently, Horn et al (11) performed multibreath ^{3}He ventilation imaging in human subjects by using a washout technique. However, as washout of the polarized gas proceeded, the signal-to-noise ratio often decreased such that only the images obtained after the first two or three breaths of the protocol were usable.

Herein, we applied the dynamic hyperpolarized gas wash-in technique to human subjects. We sought to assess the feasibility and optimize the accuracy of the multibreath wash-in hyperpolarized ^{3}He approach to ventilation measurement as well as to examine the physiologic differences that this approach reveals among nonsmokers, asymptomatic smokers, and patients with COPD.

Advances in Knowledge

- A multibreath wash-in approach for measuring regional fractional ventilation by using hyperpolarized helium 3 (^{3}He) MR imaging is both feasible and precise in human subjects, exhibiting very good agreement with an alternative global measurement in nine human subjects (relative mean difference, 2.9% ± 5.7; R^2 = 0.96); the mean overall whole-lung fractional ventilation in all subjects was 0.24 ± 0.06.
- Multibreath wash-in ventilation imaging is made feasible through the development of a gas delivery device that is compatible with MR imaging and subject-driven while delivering precise, consistent volume; gas volume delivery error is less than 50 mL per breath (5%–7% for an adult breath size) with consistent fraction of inspired oxygen.

Materials and Methods

All experiments were approved by the local institutional review board and compliant with the Health Insurance Portability and Accountability Act. Informed consent was obtained from all subjects. Subjects' vital signs were monitored throughout testing under supervision of a physician (M.D.R., with 40 years of experience). All subjects tolerated the imaging protocol well.

Subject Groups, Demographics, and Pulmonary Function Tests

Nine subjects were included in our study (mean age, 51 years; age range, 41–64 years). Subjects were classified into three groups, as follows: healthy subjects with no history of smoking (one man, two women; mean age ± standard deviation, 45 years ± 4), asymptomatic smokers (three men; mean age, 51 years ± 5; mean pack-years, 24 ± 5), and smokers with moderate COPD (three men; mean age, 59 years ± 5; mean pack-years, 38 ± 12). There were more men (n = 7; mean age, 53 years ± 7) than women (n = 2; mean age, 45 years ± 5) in this study. The two sexes in the study were not significantly different with respect to age (P = .162, Welch t test). Table 1 lists the subjects' demographics. The three cohorts were not significantly different with respect to body mass index ($F_{2,6}$ = 0.262, P = .778).

Definition of Fractional Ventilation

Fractional ventilation is a nondimensional metric for a volume element in the lung defined as the ratio of the inspired gas added to that element to the total gas space at the end of inspiration (9). Global fractional ventilation can be measured by using the ratio of the tidal volume (V_T) breathed by the subject to the total end-inspiratory volume. Signal buildup of hyperpolarized gas over a multibreath wash-in protocol can be used to calculate this parameter on a regional basis (Fig 1, Appendix E1 [online]).

Published online before print
10.1148/radiol.2015150495 **Content code:** CH

Radiology 2016; 279:917–924

Abbreviations:
COPD = chronic obstructive pulmonary disease
V_T = tidal volume

Author contributions:
Guarantors of integrity of entire study, H.H., R.R.R.; study concepts/study design or data acquisition or data analysis/interpretation, all authors; manuscript drafting or manuscript revision for important intellectual content, all authors; manuscript final version approval, all authors; agrees to ensure any questions related to the work are appropriately resolved, all authors; literature research, H.H., J.T.C., K.E., M.C., M.D.R., R.R.R.; clinical studies, H.H., S.J.K., M.C., H.S., S.S., M.D.R.; statistical analysis, H.H., M.D.R.; and manuscript editing, J.T.C., S.J.K., K.E., M.I., W.B.G., M.C., M.D.R., R.R.R.

Funding:
This research was supported by the National Institutes of Health (grant R01-HL089064).

Conflicts of interest are listed at the end of this article.

Table 1

Summary of Demographics

Subject No.	Age (y)	Sex	Smoking History (pack-years)	Height (cm)	Weight (kg)	Dead Volume (mL)*
HN1	48	F	0	156	78	116
HN2	41	F	0	160	58	125
HN3	45	M	0	189	97	189
AS1	47	M	24	179	74	166
AS2	49	M	29	178	75	162
AS3	57	M	20	173	86	151
COPD1	64	M	48	178	76	162
COPD2	55	M	40	191	105	193
COPD3	57	M	25	173	77	151

Note.—AS = asymptomatic smoker, HN = healthy nonsmoker.

* The anatomic dead volume was estimated on the basis of the subject's height.

Imaging Studies

Each subject practiced with room air until he or she could perform the multibreath protocol in the supine position. Hyperpolarized ^{3}He MR imaging was performed during seven back-to-back breath holds (the first six lasted approximately 1 second, and the final breath hold took approximately 12 seconds) after the subjects inhaled the imaging gas mixture. Subjects were instructed to inhale for 3 seconds and exhale for 4 seconds at a uniform rate to complete the seven time points.

MR imaging was performed with a 1.5-T unit (Sonata; Siemens Healthcare, Erlangen, Germany) by using an eight-channel chest coil (Stark Contrast, Erlangen, Germany). A two-dimensional gradient-echo pulse sequence with parallel imaging (generalized autocalibrating partially parallel acquisition with an acceleration factor of 4) was used for imaging with a repetition time of 6.9 msec, echo time of 3.2 msec (repetition time/echo time = 6.9/3.2), and flip angle (α) of 5°. A total of six coronal sections (section thickness = 25 mm with 20% gap) covered the whole lung with a planar resolution of 6.25 × 6.25 mm^2.

Statistical Analysis

All statistical analyses were performed by using software (R, Free Software Foundation, Vienna, Austria). Repeated measures analysis of variance was performed, followed by post hoc tests with Bonferroni correction, to assess the differences among the three cohorts. Six samples (one for each section) from each subject were compared; that is, the cohort differences were compared within each and every section in a nested design. Data are presented as means ± standard deviations. An experiment-wide type I error level of .05 was used.

Results

Signal Intensity Buildup

^{3}He spin-density buildup for representative subjects from each cohort is shown in Figure 2. In healthy subjects with no ventilation defects, the signal intensity gradually and homogeneously builds up in all voxels over the inhalations of imaging gas. In the patients who exhibit ventilation defects and voxels with very low and high signal intensity, the buildup is heterogeneous. This heterogeneity is further demonstrated in Figure 3 and Movie E1 (online), which show the section-by-section signal intensity buildup in a representative patient with COPD. Although the anterior sections are almost unventilated initially, they gradually fill completely as the protocol progresses. In the posterior sections, ventilation defects are juxtaposed with hyperinflated areas that gradually fill some adjacent regions over subsequent breaths.

Whole-Lung Fractional Ventilation

The whole-lung fractional ventilation results derived from hyperpolarized MR imaging are shown in Table 2. The whole-lung values were computed by fitting the model explained in Equation (E8) of Appendix E1 (online) to the sum of signal intensities in all voxels. The whole-lung fractional ventilation in all subjects was 0.24 ± 0.06 (range, 0.18–0.37). The ratio of administered V_T to total end-inspiratory volume, which provides an alternative measure of fractional ventilation, is also listed in Table 2. These two methods are compared in Figure 4, which represents the precision of the whole-lung fractional ventilation measurement (slope of 0.94 and negligible bias). Moreover, the two methods showed very good correlation (R^2 = 0.96, P < .001). Bland-Altman analysis also demonstrated a very good agreement between the two methods, with a relative mean difference of 2.9% and a standard deviation of ±5.7%.

Fractional Ventilation Combined with Ventilation Defects

When unventilated regions were included as zero values, the mean fractional ventilation values decreased considerably in patients with COPD and asymptomatic smokers such that a significant difference between the groups' means can be observed ($F_{2,10}$ = 7.144, P = .012) (Table 2). Post hoc tests showed a significant difference between the mean fractional ventilation of healthy subjects and patients with COPD (change = 0.091, Bonferroni P = .016) but did not show a significant difference between the asymptomatic smokers and healthy subjects (Bonferroni P = .069) or between the asymptomatic smokers and patients with COPD (Bonferroni P = .383).

Fractional Ventilation Maps

The apparent fractional ventilation maps for the middle section of two representative subjects from each

Figure 1

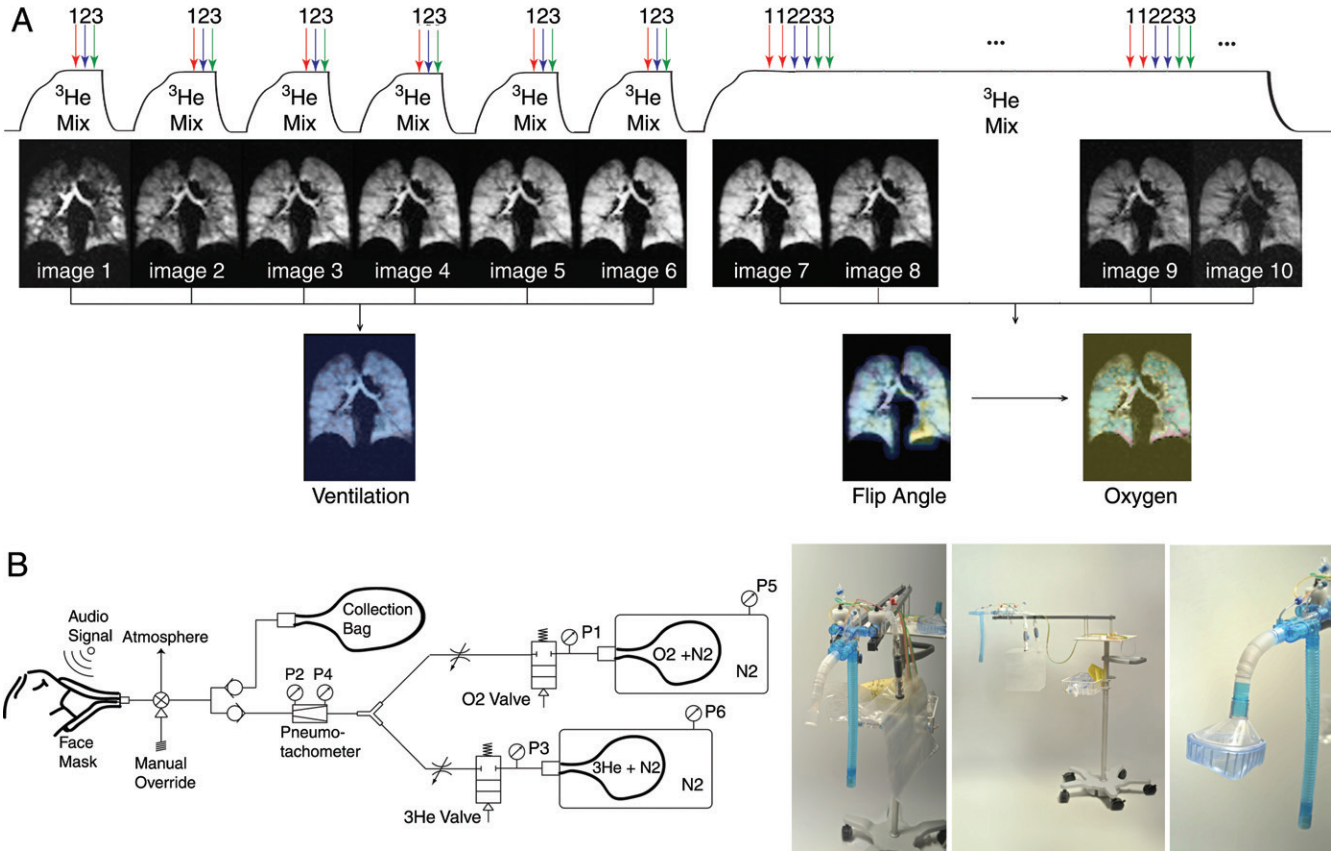

Figure 1: *A*, Multibreath sequence designed to yield quantitative measures of lung ventilation, P_{AO_2} tension, and radiofrequency depolarization. The series begins with a repeated slow inhale-exhale maneuver with an approximately 1-second multisection image acquired after each full inhale. After signal intensity buildup is complete (6–10 breaths), another last inhalation of imaging gas with an almost steady-state gas distribution is used to estimate flip angle and P_{AO_2} in a 12-second breath hold. *B*, Schematic (left) and prototype gas delivery device (right) that delivers ^3He, N_2, and O_2 at a prescribed ratio and volume by using premixed containers and measured flow. Subject breathes through mouthpiece or mask (far right); each inhalation is measured by using two pneumotachometers stopped automatically by pneumatically controlled valves at target volume. Imaging is automatically synchronized to breathing cycle. *P* = pneumotachometer.

cohort are shown in Figure 5. Healthy subjects had homogeneous maps with standard deviation (heterogeneity) of 0.036 ± 0.011 (range, 0.021–0.056). Conversely, the COPD cohort had more heterogeneous maps (mean, 0.055 ± 0.020; range, 0.031–0.089) with both hyper- and hypoventilated regions in addition to ventilation defects. The heterogeneity of fractional ventilation for all sections was significantly different among cohorts ($F_{2,10}$ = 7.639, P = .010), and the pairwise difference was significant between the healthy subjects and the patients with COPD (change = −0.019, Bonferroni P = .003) and between the healthy subjects and asymptomatic smokers (change = −0.020, Bonferroni P = .001).

Discussion

The wash-in approach developed in this study was made feasible by the development of a custom gas delivery system that enables subject-driven delivery of consistent, precise gas volumes as well as accurate monitoring of the fraction of inspired oxygen. This system facilitates an imaging scheme that approximates the physiology of natural breathing; consequently, the acquired data differ in fundamental ways from those obtained with single-breath techniques. Execution of this method revealed significant associations between increased ventilation heterogeneity and smoking, a finding that echoes those from several previous studies (12–14). It also provided the opportunity to develop several techniques for increasing the accuracy of fractional ventilation measurements.

By more closely simulating natural breathing mechanics, the multibreath wash-in scheme has an advantage over the quantification of ventilation defects with single-breath images. As evident in the representative subject with COPD, it is possible for ventilation defects identified after just one breath to persist over the course of many subsequent

Figure 2

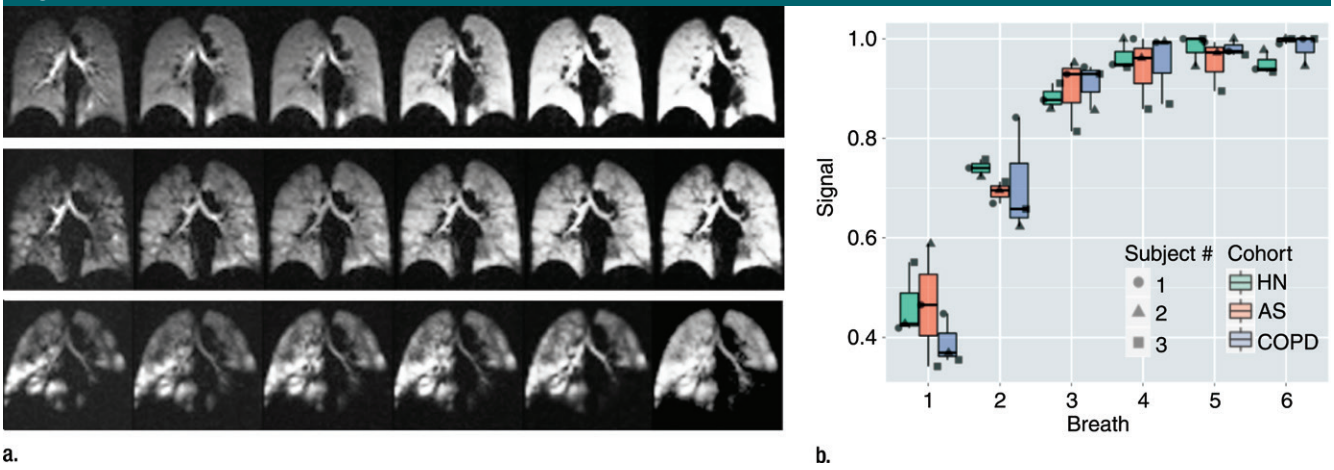

Figure 2: **(a)** MR images illustrate signal intensity buildup during repeated hyperpolarized gas breaths in healthy nonsmoker (top), asymptomatic smoker (middle), and patient with COPD (bottom) and show progression of nonuniform ventilation and apparent resolution of some (but not all) defects during an extended breathing sequence. Image sets used six breaths with an accelerated $6 \times 48 \times 64$ image acquired after each inhalation, necessitating 1.02 seconds. **(b)** Signal intensity buildup during repeated hyperpolarized gas breaths for the entire subject box plotted for each cohort. Note that whole-lung values in each breath are integration of signal intensities in all voxels in lung. For better comparison, whole-lung sum of signal intensities in each breath for each subject is normalized by maximum signal intensity observed in that subject during course of imaging (ie, breath with the highest signal intensity has a value of 1.0). *AS* = asymptomatic smokers, *HN* = healthy nonsmokers.

Figure 3

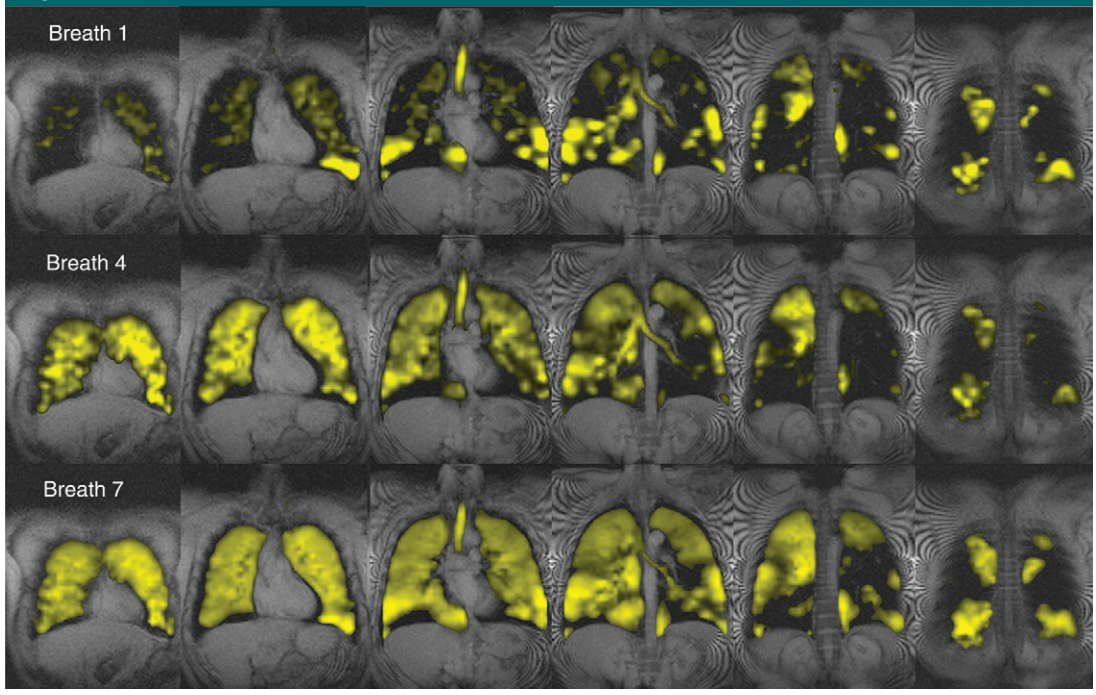

Figure 3: Images illustrate ^{3}He signal intensity overlaid on ^{1}H images of chest cavity in first (top), fourth (middle), and seventh (bottom) breath in all sections of a representative subject with stage 2 COPD. Initial signal intensity is highly inhomogeneous and characterized by a small volume of hyperventilated lung due to partial or complete obstruction in other regions. Although gas is eventually exchanged with much of the lung, abnormal tissue mechanics in these focal areas may contribute to subsequent emphysematous remodeling.

Table 2

Fractional Ventilation Results

						High-Spatial-Resolution Fractional Ventilation†		
Subject No.	V_T (mL)	EIV (L)	V_T/EIV	Whole-Lung Fractional Ventilation*	Specific Ventilation	Fractional Ventilation‡	Fractional Ventilation Heterogeneity	Ventilation Defect (%)
HN1	747	2.03	0.368	0.368	0.582	0.336 (0.093)	0.033 (0.014)	1.0 (1.0)
HN2	659	2.21	0.298	0.247	0.328	0.224 (0.049)	0.033 (0.004)	1.0 (0.8)
HN3	1036	4.39	0.236	0.194	0.241	0.193 (0.099)	0.043 (0.009)	2.0 (2.0)
Mean	814 (198)	2.88 (1.32)	0.31 (0.07)	0.27 (0.09)	0.39 (0.18)	0.251 (0.101)	0.036 (0.011)	1.3 (1.4)
AS1	679	3.22	0.211	0.181	0.221	0.154 (0.067)	0.055 (0.021)	7.0 (4.0)
AS2	641	3.62	0.177	0.177	0.215	0.159 (0.052)	0.047 (0.018)	2.7 (1.5)
AS3	866	3.07	0.282	0.282	0.393	0.250 (0.083)	0.063 (0.017)	11.5 (7.2)
Mean	729 (121)	3.31 (0.29)	0.23 (0.06)	0.22 (0.06)	0.28 (0.11)	0.188 (0.079)	0.056 (0.018)	7.1 (5.9)
COPD1	823	3.89	0.212	0.188	0.232	0.131 (0.015)	0.062 (0.018)	29.4 (20.4)
COPD2	1072	4.02	0.267	0.235	0.307	0.164 (0.040)	0.041 (0.007)	17.6 (17.4)
COPD3	821	2.83	0.290	0.291	0.410	0.186 (0.048)	0.063 (0.025)	27.1 (20.0)
Mean	906 (145)	3.58 (0.66)	0.26 (0.05)	0.24 (0.06)	0.32 (0.09)	0.160 (0.042)	0.055 (0.020)	24.7 (18.9)

Note.—AS = asymptomatic smoker, EIV = end-inspiratory volume computed from ^{3}He spin-density maps, HN = healthy nonsmoker. Specific ventilation was calculated as follows: fractional ventilation/(1 − fractional ventilation). Numbers in parentheses are standard deviations.

* Whole-lung fractional ventilation was based on fitting to the summation of all the imaged voxels' signal intensity buildup.

† High-spatial-resolution fractional ventilation was based on fitting to each voxel's signal intensity buildup.

‡ Fractional ventilation determined with unventilated regions included as zero values.

Figure 4

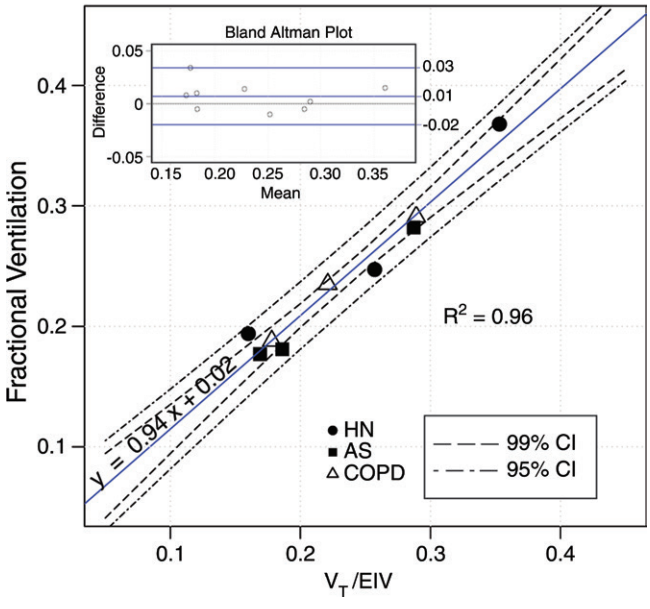

Figure 4: Graph shows comparison between whole-lung imaged fractional ventilation with ratio of V_T (measured with gas delivery system) to end-inhalation inspired volume *(EIV)* (computed from ^{3}He spin-density maps). Bland-Altman plot (inset, top left) compares the two alternative methods. *AS* = asymptomatic smokers, *CI* = confidence interval, *HN* = healthy nonsmokers.

breaths. However, apparent ventilation defects can also vary drastically according to how many breaths of imaging gas have been inhaled. In the same COPD subject, the most anterior section showed only large defects and regions of very low signal intensity after the first breath. However, by the final breath, this section is mostly ventilated and resembles the spin-density maps of a healthy subject.

Several techniques were implemented in this study to minimize error in the fractional ventilation values. An important contributor to error is the mechanical dead space wherein hyperpolarized signal is modulated by factors other than the physiologic trait under consideration. As explained by Emami et al (10), dead space is composed of both the static volume in the gas delivery line and the dynamic volume in the portion of the ventilator system after the respirator valve, the trachea, and the main bronchi. During the ventilation imaging protocol, the dynamic volume thus contains gas exhaled from the previous breath (ie, rebreathing).

Figure 5

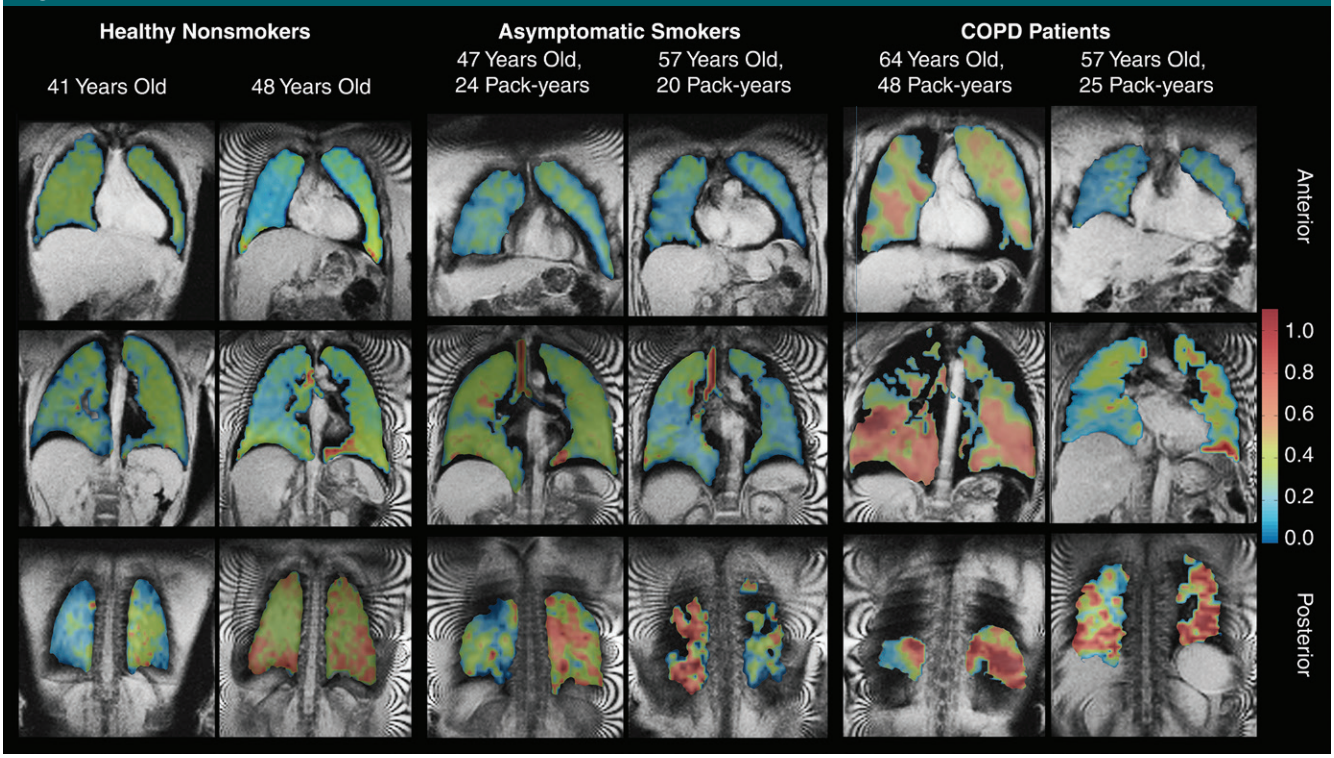

Figure 5: Representative fractional ventilation maps from two subjects in each group. The most anterior, the middle, and the most posterior sections are shown for each subject (top to bottom).

By generating models of both dead space volumes, we corrected for their contribution to global fractional ventilation. Correcting for the influence of dead space on regional fractional ventilation values is substantially more challenging because one cannot determine the destination of hyperpolarized gas rebreathed from a given voxel. As such, we used the model of apparent regional fractional ventilation used by Emami et al, which includes an offset term assumed to represent the contribution of rebreathing. Because the fractional ventilation derived from the global model developed herein and the fractional ventilation derived from the sum of the whole-lung signal intensity with the model from Emami et al should be the same, direct comparison of the two models allowed us to more accurately quantify the contribution of rebreathing at the regional level.

In addition to accounting for dead space, an important aspect of increasing the accuracy of hyperpolarized ^{3}He ventilation measurements is correcting for the contribution of oxygen to hyperpolarized signal loss. Our approach allows for the buildup of sufficient signal to calculate P_{AO_2} in the last breath, when the gas has had enough time to fill the parenchyma in those subjects with slow-filling regions. We estimated voxelwise P_{AO_2} for any time point during the course of the ventilation maneuver by calculating R (apparent rate of oxygen uptake). Without this adjustment of P_{AO_2} values, fractional ventilation would have been overestimated by approximately 10%. This approach thus builds on that of Horn et al (11), whose washout technique did not provide enough signal to directly produce a high-spatial-resolution regional P_{AO_2} map.

The above-described techniques for error correction allowed us to achieve a high accordance between whole-lung fractional ventilation measured with hyperpolarized ^{3}He and global fractional ventilation measured by using the gas delivery device turnover. The correlation between the global ventilation values obtained from the ^{3}He signal intensity and those from the gas delivery system and segmented maps was very good (R^2 = 0.96) and did not exhibit any bias. The mean global value of fractional ventilation for all subjects was 0.24 ± 0.06 (equivalent to a specific ventilation of 0.33 ± 0.12), which closely corresponds with the average global measurements reported by Sá et al (15) (specific ventilation, 0.33 ± 0.11).

The foremost limitation of this study is that the V_T of each subject during ordinary tidal breathing was not directly measured; rather, it was estimated on the basis of weight. The estimated V_T was then rounded to one of three set points to which our gas delivery system was calibrated so as to ensure precision. This shortcoming resulted from difficulties with

the linearity of the gas delivery control system outside the normal range. Consequently, in subjects with a disproportionate ratio of weight to lung volume, the whole-lung fractional ventilation values we obtained are effort-dependent rather than clinical. In addition, we did not attempt to quantify the amount of error produced by misregistration. Similarly, we assumed that ^{3}He gas was stationary during the 1-second breath hold. In the case of diseased lung with high diffusion and the possibility of collateral ventilation, this assumption may not be entirely true. This effect could account for a fraction of the heterogeneity observed in patients with COPD and asymptomatic smokers.

In conclusion, we demonstrated the feasibility of performing multibreath wash-in hyperpolarized ^{3}He MR imaging to assess regional fractional ventilation in healthy subjects and patients with COPD. By allowing the subject to drive gas delivery and proceed through several breaths, such an approach reveals spatiotemporal aspects of ventilation that are not taken into account by the quantification of ventilation defects after a single breath.

Disclosures of Conflicts of Interest: H.H. disclosed no relevant relationships. **J.C.** disclosed no relevant relationships. **S.J.K.** disclosed no relevant relationships. **K.E.** Activities related to the present article: disclosed no relevant relationships. Activities not related to the present article: is employed by Polarean; has stock/stock options in Polarean. Other relationships: disclosed no relevant relationships. **M.I.** disclosed no relevant relationships. **W.G.** disclosed no relevant relationships. **Y.X.** disclosed no relevant relationships. **M.C.** disclosed no relevant relationships. **H.S.** disclosed no relevant relationships. **S.S.** disclosed no relevant relationships. **M.R.** disclosed no relevant relationships. **R.R.R.** disclosed no relevant relationships.

References

1. Altemeier WA, McKinney S, Glenny RW. Fractal nature of regional ventilation distribution. J Appl Physiol (1985) 2000; 88(5):1551–1557.
2. Macklem PT. The physiology of small airways. Am J Respir Crit Care Med 1998; 157(5 Pt 2):S181–S183.
3. Kirby M, Pike D, Coxson HO, McCormack DG, Parraga G. Hyperpolarized (3)He ventilation defects used to predict pulmonary exacerbations in mild to moderate chronic obstructive pulmonary disease. Radiology 2014;273(3):887–896.
4. Tustison NJ, Altes TA, Song G, de Lange EE, Mugler JP III, Gee JC. Feature analysis of hyperpolarized helium-3 pulmonary MRI: a study of asthmatics versus nonasthmatics. Magn Reson Med 2010;63(6):1448–1455.
5. Kirby M, Svenningsen S, Ahmed H, et al. Quantitative evaluation of hyperpolarized helium-3 magnetic resonance imaging of lung function variability in cystic fibrosis. Acad Radiol 2011;18(8):1006–1013.
6. O'Sullivan B, Couch M, Roche JP, et al. Assessment of repeatability of hyperpolarized gas MR ventilation functional imaging in cystic fibrosis. Acad Radiol 2014;21(12):1524–1529.
7. Lee EY, Sun Y, Zurakowski D, Hatabu H, Khatwa U, Albert MS. Hyperpolarized 3He MR imaging of the lung: normal range of ventilation defects and PFT correlation in young adults. J Thorac Imaging 2009;24(2):110–114.
8. Marshall H, Deppe MH, Parra-Robles J, et al. Direct visualisation of collateral ventilation in COPD with hyperpolarised gas MRI. Thorax 2012;67(7):613–617.
9. Deninger AJ, Mansson S, Petersson JS, et al. Quantitative measurement of regional lung ventilation using 3He MRI. Magn Reson Med 2002;48(2):223–232.
10. Emami K, Kadlecek SJ, Woodburn JM, et al. Improved technique for measurement of regional fractional ventilation by hyperpolarized 3He MRI. Magn Reson Med 2010;63(1):137–150.
11. Horn FC, Deppe MH, Marshall H, Parra-Robles J, Wild JM. Quantification of regional fractional ventilation in human subjects by measurement of hyperpolarized 3He washout with 2D and 3D MRI. J Appl Physiol (1985) 2014;116(2):129–139.
12. Anthonisen NR, Bass H, Oriol A, Place RE, Bates DV. Regional lung function in patients with chronic bronchitis. Clin Sci 1968;35(3):495–511.
13. Gaziano D, Seaton A, Ogilvie C. Regional lung function in patients with obstructive lung diseases. BMJ 1970;2(5705):330–333.
14. Vidal Melo MF, Winkler T, Harris RS, Musch G, Greene RE, Venegas JG. Spatial heterogeneity of lung perfusion assessed with (13)N PET as a vascular biomarker in chronic obstructive pulmonary disease. J Nucl Med 2010;51(1):57–65.
15. Sá RC, Cronin MV, Henderson AC, et al. Vertical distribution of specific ventilation in normal supine humans measured by oxygen-enhanced proton MRI. J Appl Physiol (1985) 2010;109(6):1950–1959.doi:10.1152/japplphysiol.00220.2010 PubMed.